



A double-dichotomy clustering of dual pathology dementia patients

Arvind Caprihan^{a,*}, Rajikha Raja^{a,d}, Laura J. Hillmer^b, Erik Barry Erhardt^c, Jill Prestopnik^b, Jeffrey Thompson^b, John C Adair^b, Janice E. Knoefel^b, Gary A. Rosenberg^b

^a The Mind Research Network, Albuquerque, NM, United States

^b Department of Neurology, University of New Mexico, Albuquerque, NM, United States

^c Departments of Mathematics and Statistics, University of New Mexico, Albuquerque, NM, United States

^d Department of Radiology, University of Arkansas for Medical Sciences, Little Rock, AR, United States

ARTICLE INFO

Keywords:

Dual pathology dementia
Double-dichotomy clustering
White matter
Mean diffusivity
Amyloid
Phosphorylated Tau

ABSTRACT

Introduction: Subcortical ischemic vascular disease (SIVD) and Alzheimer's disease (AD) related dementia can coexist in older subjects, leading to mixed dementia (MX). Identification of dementia sub-groups is important for designing proper treatment plans and clinical trials.

Method: An Alzheimer's disease severity (ADS) score and a vascular disease severity (VDS) score are calculated from CSF and MRI biomarkers, respectively. These scores, being sensitive to different Alzheimer's and vascular disease processes are combined orthogonally in a double-dichotomy plot. This formed an objective basis for clustering the subjects into four groups, consisting of AD, SIVD, MX and leukoaraiosis (LA). The relationship of these four groups is examined with respect to cognitive assessments and clinical diagnosis.

Results: Cluster analysis had at least 83% agreement with the clinical diagnosis for groups based either on Alzheimer's or on vascular sensitive biomarkers, and a combined agreement of 68.8% for clustering the four groups. The VDS score was correlated to executive function ($r = -0.28, p < 0.01$) and the ADS score to memory function ($r = -0.35, p < 0.002$) after adjusting for age, sex, and education. In the subset of patients for which the cluster scores and clinical diagnoses agreed, the correlations were stronger (VDS score-executive function: $r = -0.37, p < 0.006$ and ADS score-memory function: $r = -0.58, p < 0.0001$).

Conclusions: The double-dichotomy clustering based on imaging and fluid biomarkers offers an unbiased method for identifying mixed dementia patients and selecting better defined sub-groups. Differential correlations with neuropsychological tests support the hypothesis that the categories of dementia represent different etiologies.

1. Introduction

The two most common forms of dementia, Alzheimer's disease (AD) and vascular cognitive impairment and dementia (VCID) are prevalent among the aging population. VCID is a heterogeneous brain disorder that accounts for 20% of dementia cases and is second in occurrence to AD [1]. Both AD and VCID can depend on multiple factors and are broad disease processes leading to dementia. In this paper we study subjects with subcortical ischemic vascular disease (SIVD), a small vessel form of VCID characterized by vascular white matter damage and neuroinflammation [2], and AD subjects characterized by amyloid deposition (A), tau pathology (T), and neurodegeneration (N) [3,4]. Although AD pathology is different from cerebrovascular pathology leading to VCID, the two disease processes frequently occur together in a population over 65 years of age [5], leading to what is called mixed dementia (MX).

White matter damage as characterized by white matter hyperintensities (WMHs) in FLAIR images and mean diffusivity measured by the peak skeletonized mean diffusivity (PSMD) are considered as markers of ischemic cerebral small vessel disease [6–9]. It is also well recognized that in older populations white matter damage, which is a marker of SIVD can occur together with AD markers of increased amyloid and phosphorylated tau (pTau) deposition [5]. There is a continuing debate on the relationship between white matter damage markers and the AD-factors: are they independent factors causing mixed dementia, or are they acting synergistically with one influencing the other [10]. There are also recent studies that have found association between the regional locations of WMH and amyloid deposition [11,12]. In these same studies, the relationship between WMHs and pTau was weaker. There was no global or voxel-based association between pTau with WMH burden, but some regional association of lower pTau concentration with WMHs lo-

Abbreviations: AD, Alzheimer's disease; SIVD, Subcortical ischemic vascular disease; LA, Leukoaraiosis; MX, Mixed Dementia; WMH, White Matter Hyperintensity; PSMD, Peak width of skeletonized mean diffusivity; ADS, Alzheimer's disease severity; VDS, Vascular disease severity; pTau, Phosphorylated Tau.

* Corresponding author.

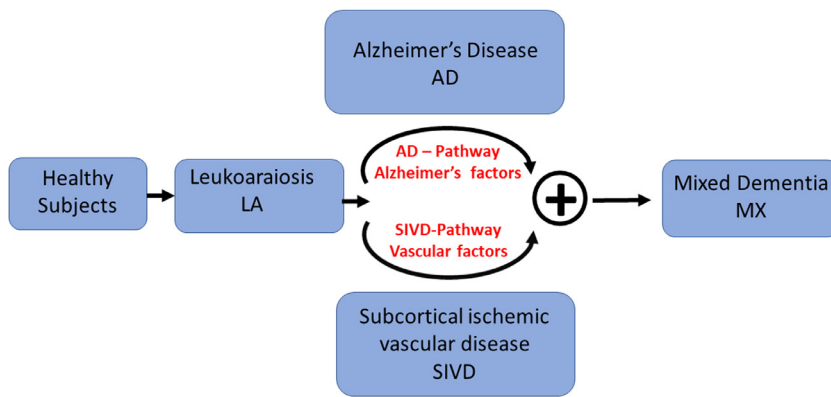
E-mail address: acaprihan@mrn.org (A. Caprihan).

<https://doi.org/10.1016/j.cccb.2021.100011>

Received 16 January 2021; Received in revised form 22 March 2021; Accepted 27 March 2021

Available online 2 April 2021

2666-2450/© 2021 The Authors. Published by Elsevier B.V. This is an open access article under the CC BY-NC-ND license (<http://creativecommons.org/licenses/by-nc-nd/4.0/>)



cations was found. This is slightly contradictory because a higher pTau concentration is an AD marker. In this study we recognize that white matter damage can occur concurrently with AD pathology and attempt to identify these MX subjects.

Fig. 1 describes the transition of healthy subjects to MX through a dual-pathway model [13]. Fig. 1 also introduces a group of subjects we call leukoaraiosis (LA), which are typically cognitively normal but have some radiographic white matter damage. Some of the LA subjects can with neurodegeneration become AD-like while others with neuroinflammation be more SIVD-like. At an older age the two disease processes can be concurrently present in subjects and they are said to have MX. We develop a biological biomarker-based strategy to identify MX subjects. The LA subgroup is not a dementia subtype, it is thought to be a precursor to AD, SIVD, and MX. The disease progression model of Fig. 1 is a conjecture and we do not address its validity because this is not a longitudinal study. A longitudinal study has examined the evolution of AD and VCID trajectories in the Danish National Patient Registry [14]. They found that before dementia diagnosis both disease trajectories were similar, making early diagnosis difficult. Unlike their study, we evaluate the combined occurrence of AD and VCID in a cross-sectional study based on imaging and fluid biomarkers. The takeaway points for this paper is that AD and SIVD pathways are two independent processes and in older subjects they can occur independently or concurrently.

There is an interest in developing biomarkers for the spectrum of neurodegenerative diseases because of the need for early diagnosis followed by early treatment. Biomarkers also provide outcome measures for evaluating treatment efficacy and disease progression. In addition, biomarkers afford a more reproducible definition of the disease which can be uniformly applied across multiple sites. The two separate disease processes suggest that the biomarkers for each pathway can also be found separately. Here we propose that vascular disease severity (VDS) score and an Alzheimer's disease severity (ADS) score can be found corresponding to each pathway, based on the corresponding biomarkers. The biomarkers for the two pathways are expected to be different but can overlap. In this paper for illustration purposes, we just use two biomarkers for each score. One could use more biomarkers as appropriate. The VDS score is based on white-matter hyperintensity volume calculated from a FLAIR image and the peak width of skeletonized mean diffusivity (PSMD) [8] calculated from the mean-diffusivity image. The ADS score is calculated based on the CSF markers of $A\beta$ Ratio = $A\beta_{42}/A\beta_{40}$ and pTau. Fig. 2 illustrates our concept of calculating the two severity scores.

The dual-pathology model leads to a double-dichotomy clustering method to identify the four groups (LA, AD, SIVD, and MX). The VDS and ADS scores are respectively plotted orthogonally on the x-axis and the y-axis to give a two-dimensional scatter plot. The position of a subject on this plot gives information on the disease severity and the disease type. Fig. 3 shows an idealized scatterplot of ADS against VDS. We can divide each axis into two parts with a cut-off of 0.5, to define two sepa-

rate groups, VDS^- and VDS^+ , as those with low and high vascular damage, and ADS^- and ADS^+ groups with low and high AD severity. This yields four cluster (c) groups ($cMX = VDS^+ADS^+$, $cSIVD = VDS^+ADS^-$, $cAD = VDS^-ADS^+$, and $cLA = VDS^-ADS^-$) analogous to those defined on the basis of clinical diagnosis (MX, SIVD, AD, LA). An advantage of continuous numerical scores is that the location of the subject on this 2D-scatter plot describes disease severity. For example, subject(a) is classified as cMX, but being close to the ADS boundary, we know that its ADS factors are similar to those of SIVD subjects.

One goal of the double-dichotomy analysis is to provide a mathematical framework for diagnosing MX subjects based on objective biomarkers when the subject population includes both AD and SIVD subjects. To accomplish this, we compare agreement between the cluster and clinical diagnoses in the four groups. We also show that cluster diagnosis can be used to select a smaller group of subjects with stronger correlation with cognition. The concept of dual-dichotomy is based on the idea of condensing the wide number of available MRI and fluid biomarkers into two measures, one which reflects VDS and the other ADS. In large autopsy series, many patients show both AD and vascular pathology, making MX the most common form of dementia [15–19]. The proposed method of identifying homogenous dementia subgroups can be further validated against existing databases, such as Alzheimer's disease neuroimaging initiative (ADNI), where MRI and CSF-fluid biomarkers have been collected.

In this study we propose that vascular disease severity and Alzheimer's disease severity biomarkers can be found independently and then plotted orthogonally to get a visual description of the presence of each disease process. The example chosen in this paper to illustrate this concept is based on accepted measures of cerebral small vessel disease and AD pathology. WMHs are typically associated with vascular problems and in the present study, rather than just consider WMH we have included information from mean diffusivity images to define white matter damage. The VDS and ADS scores are also related to executive and memory function to understand their biological relevance.

2. Method

2. Method

2.1. Study participants

The University of New Mexico (UNM) Cohort contains 184 subjects, with 94 subjects diagnosed with VCID and 55 healthy controls (HCs). Informed consent of the UNM approved IRB protocol was obtained from all subjects. The patients were classified into four categories, SIVD, AD, MX, and LA, through consensus diagnosis of three neurologists based on accepted clinical guidelines (Table 1). SIVD is the small vessel form of VCID. It is characterized by progressive growth of MRI white matter hyperintensity (WMH). SIVD patients met both the Erkinjuntti[20] criteria for subcortical vascular dementia and the recent consensus statement for SIVD [21,22]. Patients diagnosed with AD presented with a

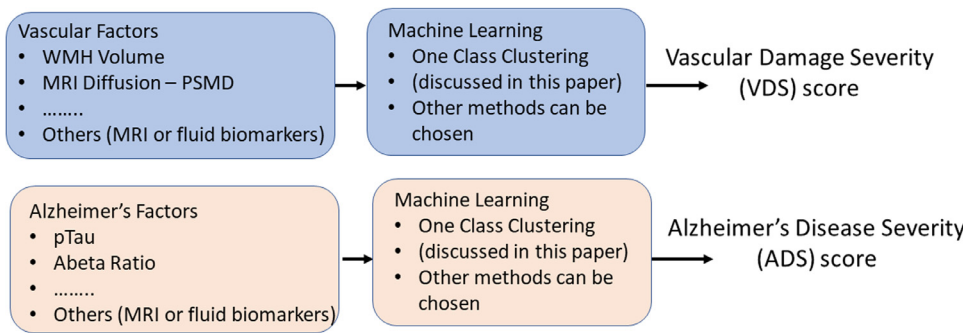


Fig. 2. A method to calculate a normalized vascular damage severity (VDS) score and an Alzheimer's disease severity (ADS) score based on vascular and Alzheimer's factors is presented. We illustrate this general concept based on two vascular factors, consisting of white matter hyperintensity (WMH) volume and the peak width skeletonized mean diffusivity (PSMD) measured from the diffusion image, and two Alzheimer's factors, consisting of Aβ Ratio and pTau. These two factors are then used to generate a VDS score and the ADS score in the range (0,1), based on the one class clustering method.

Table 1
Definitions used for creating patient subgroups based on clinical, MRI and CSF fluid markers.

Diagnoses	Description
Subcortical ischemic vascular disease (SIVD)	SIVD is the small vessel form of VCID. It is diagnosed by a progressive growth of the WMHs. They met both the Erkinjuntti [20] criteria for subcortical vascular dementia and the recent consensus statement for SIVD [21,22]
Alzheimer's disease (AD)	Patients diagnosed with AD presented with insidious onset of predominant amnesic disorder associated with one additional cognitive domain, following NINCDS-ADRDA clinical criteria for probable AD [23,24]. In addition, they conformed to the recent biological diagnostic criteria for AD [3], which includes the biomarkers of the AD pathophysiological process, low CSF Aβ42/Aβ40 and elevated phospho-Tau.
Mixed dementia (MX)	MX is diagnosed by a combination of CSF biomarkers for AD and white matter injury markers of SIVD derived from diffusion tensor imaging [17,18].
Multiple infarcts (MI)	MI patients have multiple strokes, generally involving large vessels, but it also includes isolated lacunar strokes confined primarily to thalamus or basal ganglia (single strategic strokes) [46]
Leukoaraiosis (LA)	LA is diagnosed by a combination of white matter changes on FLAIR MRI but without the evidence of dementia and minimal or no cognitive changes on neuropsychological testing. This use of the term follows the original intent of Hachinski [25] and has no connotations of pathological implications.

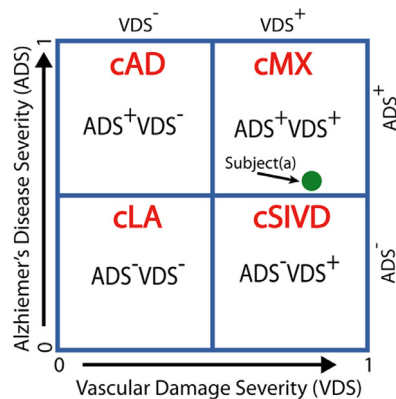


Fig. 3. The double-dichotomy clustering method is a two-dimensional scatter plot with the x-axis being the VDS score and the y-axis being the ADS score, and a cut-off of 0.5 for each axis gives four quadrants, with each quadrant describing subjects with different disease characteristics. The four cluster (c)-based patient groups are cLA = VDS⁻ADS⁻, cAD = VDS⁻ADS⁺, cSIVD = VDS⁺ADS⁻, and cMX = VDS⁺ADS⁺. The location of a subject on this plot describes disease severity. For example, subject(a) is classified as cMX, but being close to the ADS boundary, we know that its ADS factors are similar to some of the SIVD subjects.

predominantly amnesic disorder with at least one additional cognitive deficit and met DSM-V criteria for dementia. Patients with AD also met NINCDS-ADRDA clinical criteria for probable AD [23,24]. MX was diagnosed for patients with clinical features of AD combined with history of vascular risk factors, neurologic exam abnormality and moderate-severe WMH (Fazekas scale >1). LA was diagnosed in patients with white matter changes on FLAIR, low PSMD, normal neurologic exam, no evidence of dementia and only minimal cognitive changes [25]. Subjects with multiple infarcts were excluded from this study.

2.2. MRI biomarkers

All MRI scans are performed on a Siemens 3T TRIO scanner with a 12-channel radio frequency (RF) coil and later with a 32-channel RF coil. The T1-weighted and the FLAIR image had 1 mm isotropic resolution with 192 slices for both the RF coils. The diffusion tensor image (DTI) had 2 mm isotropic resolution with 72 slices. On the 12-channel coil, the diffusion protocol had a single-shell of b-value = 800 s/mm² and 30 different gradient directions, while on the 32-channel coil a multi-band sequence with three shells was used. A single b-value shell with 55 gradient directions of b-value = 800 s/mm² or b-value = 1000 s/mm² was extracted for this study.

FLAIR images were segmented and WMH volumes calculated using the IDEALab software (<https://ideallab.ucdavis.edu/>). The diffusion data were motion and eddy-current corrected based on FSL and the mean-diffusivity calculated. The PSMD was calculated based on the publicly available scripts [8].

We had a complete set of MRI and cognitive biomarkers on all subjects, and a complete set of CSF values on 80 subjects. The WMH volume was converted to a log scale before converting it to a Z-score. Conversion to Z-scores removes bias and adjusts for variability across different measurement methods. After converting to Z-scores, the PSMD biomarker in the healthy control group showed no significant statistical difference between measurements made with different RF coils.

2.3. CSF biomarkers

The two CSF fluid biomarkers used for this analysis were Tau protein phosphorylated at serine position 181 (pTau), and amyloidβ₁₋₄₂/amyloidβ₁₋₄₀ ratio (Aβ42/Aβ40 or Aβ-ratio). Amyloid was measured by ELISA with Meso Scale Discovery kits and pTau by Fujiribio ELISA. The control CSF was obtained from spinal anesthesia patients undergoing orthopedic surgery. The CSF controls were a different group of subjects than the controls for MRI and cognitive assessments. The control subjects are only used to get the base line values for

Table 2
Subject demographics and biomarker for healthy controls and the four patient groups.

	HC	LA	AD	SIVD	MX	Total Patients
Subjects with MRI data	55	20	35	23	16	94
Subjects with CSF data	51	16	30	18	16	80
Age $\mu(\sigma)$ Range	65.7 (9.6)[50,93]	62.8 (9)[44,82]	69.6 (8.3)[52,84]	67.4 (8.2)[46,83]	75.5 (3.8)[69,83]	68.6 (8.8)[44,84]
Gender (M:F)	27:28	6:14	19:16	11:12	10:6	46:48
WMH Volume $\mu(\sigma)$	3.3xE3(4.7xE3)	1.4xE4(1.0xE4)	0.7xE4(0.7xE4)	3.8xE5(2.9xE5)	3.2xE5(2.4xE5)	2.04xE4(2.3xE4)
Log10(WMH Vol) $\mu(\sigma)$	3.22 (0.399)	4.02(0.36)	3.58(0.73)	4.47(0.33)	4.36(0.41)	4.02(0.65)
PSMD $\mu(\sigma)$	0.00028(4E-05)	0.00035(6.7E-05)	0.00035(9.7E-05)	0.00050(1.3E-04)	0.00052(1.4E-04)	0.00042(1.3E-04)
A β Ratio $\mu(\sigma)$	0.092 (0.021)	0.089(0.022)	0.049(0.023)	0.074(0.028)	0.041(0.02)	0.061(0.03)
pTau $\mu(\sigma)$	54.42(12.22)	48.7(14.34)	94.1(38.4)	53.3(30.4)	96.6(58.5)	76.2(44.2)
Executive function $\mu(\sigma)$	50.4(4.66)	47.3(7.4)	44.3(8.0)	39.8(7.3)	41.3(4.5)	43.3(7.7)
Memory function $\mu(\sigma)$	54(8.81)	48.1(10.2)	30.6(10.1)	44.8(10.3)	32.3(9.2)	38.1(12.6)

converting to Z-scores and for the one-class clustering (OCC) algorithm. The control subjects are not used in comparing the clustering diagnosis to the clinical diagnosis or for the relationship between cognition and the severity scores.

2.4. Cognitive assessments

Cognitive tests were administered by a trained research psychologist (JP) or psychometrician and scored according to standard procedures. Standardized (T) scores were calculated for each test using published norms for each test. The exact tests for each participant varied slightly depending on the testing situation (some missing values existed for individual participants). Tests in each domain were categorized based on widely used definitions [26, 27]. Tests for memory function composite included: a) Hopkins Verbal Learning (HVL-R) [28], b) Craft story recall [29,30], and c) Rey Complex Figure Test (Long Delay) [31]. Tests for executive function included: a) Digit Span backwards [29, 30,32], b) Phonemic fluency (FAS words) [33], and c) Trail making test part B [29,30,34]. Control participants for the MRI studies underwent the same neuropsychological test battery. Although each individual T-score is standardized to mean = 50 and standard deviation = 10, we transformed the composite T-scores to Z-scores based on our control subject's values.

2.5. Data visualization

The number of subjects in each of the subgroups along with their demographics and biomarker values are given in Table 2. Fig. 4 is a two-dimensional scatter plot giving a qualitative visual summary of our data set. We just show the two biomarkers in each pathway considered for OCC and the two main cognitive functions that were tested for correlation with ADS and VDS scores. The WMH volume was normalized to the subject's intra-cranial volume, and then scaled back to the mean intra-cranial volume of the controls. A logarithm of the WMH was taken to convert the positive-skew distribution to be more normal like. All the four variables considered for OCC and the two outcome variables were converted to Z-scores based on the mean and the standard deviation of the control group. The expected difference in the different groups are seen in this figure and Table 2. We observe that a) the LA group is similar to HC controls in cognition and Alzheimer's factors (A β Ratio and pTau) and had slightly higher vascular factors (WMH volume and PSMD) than the HC group, b) the LA and AD group have similar vascular factors and the SIVD and MX group have similar vascular factors, c) the LA and the SIVD groups have Alzheimer's factors closer to those of controls, while the AD and the MX group have similar values, d) the memory is lower in AD and MX groups relative to SIVD and the LA groups, while the executive function does not separate well the four groups, but is lower in the SIVD group, and e) the two factors in each group are correlated to each other. This confirms that VDS factors separates the subjects into two groups LA+AD and SIVD+MX, while the ADS factors separates the

subjects into the two LA+SIVD and AD+MX groups. Our data supports the double-dichotomy proposed in Fig. 3.

2.6. One-class clustering

A simple one-class clustering (OCC) method [35,36], with two biomarkers in each of the AD and the SIVD pathways is used to calculate the VDS and the ADS scores (Fig. 2). Our method belongs to the class of OCC methods [35], used for outlier or novelty detection. There are several OCC methods available in PyOD (<https://pypi.org/project/pyod/>), a Python package for outlier detection [37]. We give here results based on the minimum covariance determinant (MCD) method [38], with some minor modifications. We use two VDS biomarkers, consisting of WMH volume and PSMD and two ADS biomarkers, consisting of phosphorylated tau (pTau), and A β 42/A β 40 ratio.

We chose the minimum covariance determinant (MCD), with minor modification, as the OCC method for outlier detection. The MCD method works well with elliptically symmetric unimodal distributions for the reference class. In our case this condition is satisfied for the healthy control group, which should be true in other applications for those with mild cognitive impairment.

The MCD method is based on calculating the Mahalanobis distance (MD) between the sample and the one-class distribution.

$$MD(x) = \sqrt{(x - m)^T R^{-1} (x - m)}$$

where m and R are robust estimates of the mean and covariance of the one class distribution [38]. The MD(x) is like a generalized Z-score in the multivariate space. It calculates the distance of the sample to the mean location of the reference class cluster, after accounting for the variance, and the correlation between the different features. The MCD method introduced the concept of robust mean and covariance estimates. This was done because the one-class data can also have outliers, and if they are included in calculation of the mean and the covariance then the sensitivity of the MD(x) is reduced. The MCD method uses a subset h of n observations to calculate m and R . A subset is chosen which gives the minimum determinant of R . After the subset has been selected MD can be calculated for all the data points. In order to detect outliers a threshold is still needed to decide if a sample is an outlier. A contamination factor in the MCD algorithm, which is the percentage of outliers in the reference class, determines the threshold. The default contamination factor of 0.1 was used.

We modified the MCD method for our application. An outlier, as detected by the MCD method can be different from the reference set as having disease severity much higher than the reference set or much lower than the reference set. We are only interested in high disease severity outliers. In other words, we need a one-sided statistical test and the MD(x), being a magnitude, does not give us directional information. We define a signed MD(x), with positive outlier distance indicating greater disease severity. We transform the observed correlated biomarkers to being uncorrelated, and calculate the mean severity index after correcting individually the sign of each biomarker. In

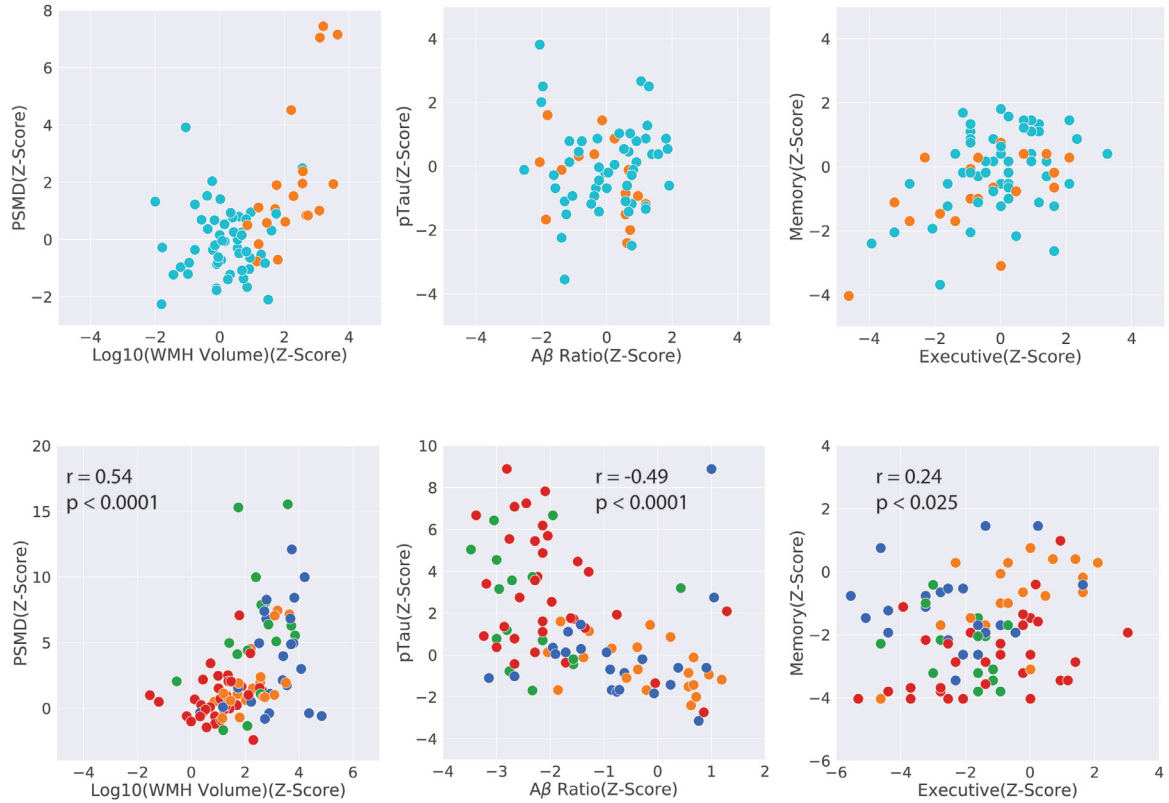


Fig. 4. This figure qualitatively compares the vascular factors (WMH volume and PSMD), the Alzheimer’s factors ($A\beta$ Ratio and pTau), and the cognition outcome measures (executive and the memory function) for the HC and the LA group in the top row and the four patient groups (LA, AD, SIVD, and MX) in the bottom row. The top row shows the similarity of LA and the healthy control group. The bottom row shows that the MRI biomarkers group AD and LA together, while the CSF biomarkers groups AD and MX together. Memory is lower in AD and MX subjects, while the executive function is lower in SIVD subjects. In the patient groups, each pair of variables is significantly correlated to the other variable. Spearman correlations and their significance is indicated.

other words, if $x = col(x_1, x_2, \dots, x_n)$ is an observation with n biomarkers, $y = R^{-1/2}x$ gives the uncorrelated biomarkers, and we calculate $\beta = u^T y = u^T R^{-1/2}(x - m)$, where $u = col(u_1, u_2, \dots, u_n)$, with $u_i = 1$, if a higher biomarker value indicates greater disease severity, and $u_i = -1$, if higher biomarker value indicates lower disease severity. β is the sum of the individual biomarkers with corrected sign. The corrected $MD_c(x) = MD(x)sgn(\beta)$.

Next to make the distance easier to interpret, we normalize $MD_c(x)$ to a variable in the range (0,1), with the additional constraint that ranking of the observations based on $MD_c(x)$ are maintained after converting to a normalized score, and the threshold of the clustering algorithm is mapped to 0.5. After normalization, an observation with a normalized score greater than 0.5 is an outlier and a score less than 0.5 is similar to the reference class. This exact choice of the mapping function is flexible. A simple choice would be a linear mapping. We have chosen a S-shaped mapping with the constraint that 10% of the patients have a score less than 0.1, and 10% have scores greater than 0.9. The mathematical form of the function was,

$$f(x) = \begin{cases} 0.5 + 0.5\text{erf}\left(\frac{(x - th)/\sigma_1}{\sigma_1}\right), & \text{for } x < th \\ 0.5 + 0.5\text{erf}\left(\frac{(x - th)/\sigma_2}{\sigma_2}\right), & \text{for } x \geq th \end{cases}$$

where σ_1 is defined by the condition that 10% of the patients are less than 0.1, and σ_2 by the condition that 10% of the patients are above 0.9. This specification can be changed to give a uniform distribution of the subjects in the range (0,1). The S-shapes curve is not symmetric around $x = th$, because $\sigma_1 \neq \sigma_2$. This is intentional because the range of OCC scores for patients has a greater variability above the MCD threshold, then below it.

Fig. 5 shows the different steps of the OCC algorithm based on the AD-pathway data. The tolerance ellipse ($\sqrt{\chi^2_{2,0.95}}$ contour) is larger

for the sample estimator than the robust estimator (Fig. 5A). The robust estimator removes outliers and gives a tighter covariance estimate. Fig. 5B shows the contour plots for the normalized ADS scores, and the ADS = 0.5 black boundary distinguishing the low and high ADS regions for the standard MCD algorithm in the Python PyOD package. The change in the contour plots and the decision boundary because of the modification of having a signed distance measure is shown in Fig. 5C. Subject(a) is close to the boundary of low and high ADS score in Fig. 5B. but it is clearly a healthy subject because pTau is negative and $A\beta$ Ratio is positive. The OCC distance measure ($MD(x)$) is inverted in sign and then normalized, which changes its ADS score to a low value close to zero.

2.7. Statistical methods

A linear regression model was used to test the association between the cognitive domains of memory and the executive function with the ADS and VDS scores after adjusting for age, sex, and education. The cognitive scores were the dependent variable and the severity scores, age, sex, and education were the independent variables. The effect of age, sex, and education was removed from the cognitive scores to calculate the residual. Pearson and Spearman correlations were calculated between the severity scores and the residual.

3. Results

3.1. Two group occ for SIVD and AD pathways

The first step of our method is the independent clustering of the VDS and ADS biomarkers into two groups each. Cluster plots for individual

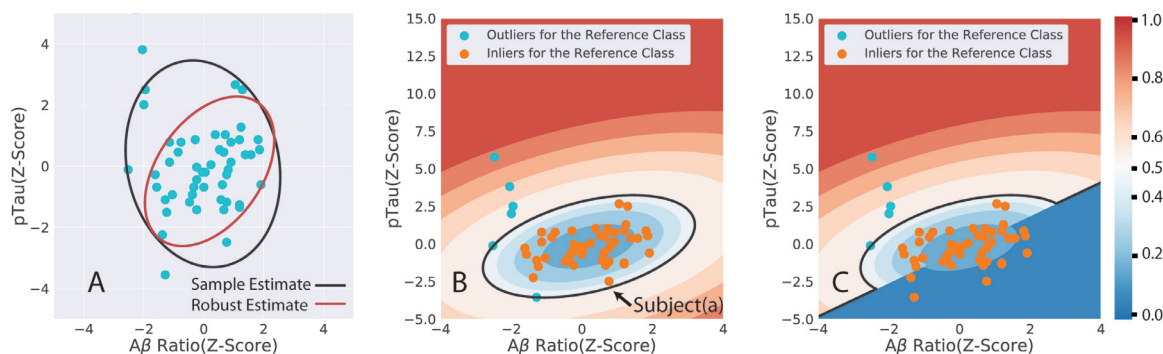


Fig. 5. The first step of minimum covariance determinant OCC algorithm is to calculate a robust mean and a covariance estimate. The tolerance ellipses (black for sample estimates and the red for the robust estimate) at $\sqrt{\chi^2_{2,0.95}}$ are shown in Fig. 5A. The robust estimator gives a tighter tolerance ellipse. Fig. 5B depicts the results of the minimum covariance determinant OCC algorithm with scores mapped to the range (0,1). The score values for any specific pTau and Aβ Ratio (Z-Scores) can be calculated from the underlying contour graph. The black contour is the 0.5 boundary between low and high scores. Fig. 5C is the modified method with OCC scores being given a positive or a negative sign before normalization. Subject(a) is close to the boundary, but it is a normal subject, and after modification it has a low normalized score.

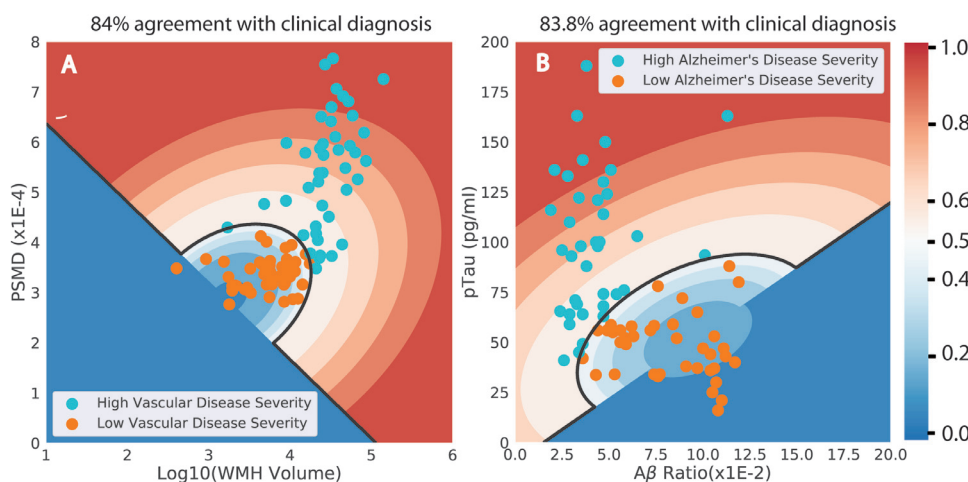


Fig. 6. The individual one-class clustering results for the two pathways are shown in terms of the measured variables. Although the clustering was done in terms of Z-scores, these figures are plotted in terms of measured variables. The dark black line is the decision boundary (score = 0.5) between the low and high severity regions. The high severity region is marked by five contours in red ranging from 0.5 to 1.0 and similarly the low severity regions has blue contours ranging from 0.0 to 0.5. Thus, knowing the values of the two variables, it is possible to evaluate the corresponding severity score.

Table 3
OCC clustering results for the AD and the SIVD pathways.

VDS variables		Two Group Agreement rate	ADS variables		Two Group Agreement rate
WMH volume	PSMD	84.0	Aβ-Ratio	pTau	83.8
WMH volume	None	80.8	Aβ-Ratio	None	77.5
PSMD	None	77.7	pTau	None	71.25

one-class clustering results for the two pathways are shown in Fig. 6. These are similar to Fig. 5C, but while Fig. 5C was in terms of the Z-Scores these plots are in terms of the original measured values. It is possible to calculate the normalized scores from these plots from the biomarker values without converting them to Z-Scores. The black line (score = 0.5) is the decision boundary between the low severity (blue) and high severity regions (red).

The agreement between the cluster and the clinical groups was 84% for the SIVD-pathway groups and 83.8% for the AD-pathway groups. The cluster groups for each pathway are $VDS^- = cLA+cAD$, $VDS^+ = cSIVD+cMX$, $ADS^- = cLA+cSIVD$, and $ADS^+ = cAD+cMX$. If only one biomarker is used instead of the two used here, the agreement with the clinical diagnosis reduces, as expected. Table 3 shows that the agreement rates for the AD and SIVD pathways when two or only one individual biomarker is used. The agreement between cluster and clinical diagnosis for the VCID-pathway is 80.8% with only WMH volume and 77.7% with only PSMD. Similarly, the agreement between cluster and clinical diagnosis for the AD-pathway is 77.5% with only Aβ ratio and 77.7% with only pTau.

The clinical diagnosis of the misclassified subjects was informally reexamined to consider which factors contributed to incongruence with the cluster designation. The disagreements occurred when the two biomarkers in each category did not indicate the same diagnosis, and clinical exam and/or cognition was a factor in decision making.

3.2. Double-dichotomy clustering for four patient groups

The normalized individual pathway clusters scores are displayed as scatter plots in Fig. 7. A cut-off = 0.5 separates the four groups along each pathway. Each cluster group lies in a separate quadrant. A continuous measure of disease severity is obtained from the subject's location in the 2D-scatter plot. Table 4 gives the four group agreement between mismatch confusion matrix with an overall accuracy of 68.8%. The poorest agreement was in classifying AD subjects. Six of the clinically diagnosed AD subjects were classified as cLA and five as cMX.

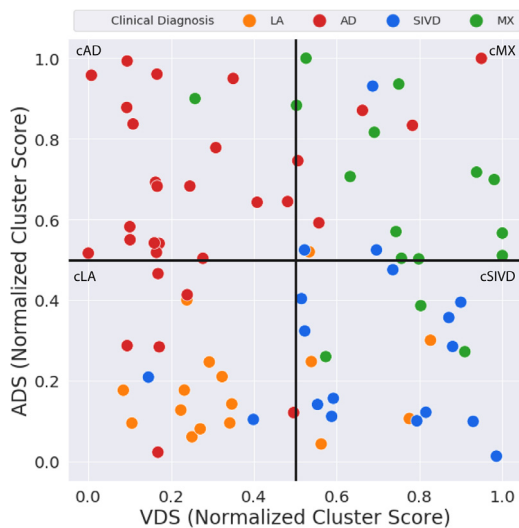


Fig. 7. The results of the two individual pathway analysis are combined into a two-dimensional scatter plot and the cluster diagnoses is compared to the clinical diagnoses. There are 80 subjects in this analysis and the cluster diagnosis agreement to the clinical diagnosis is 68.8%, or in 55 subjects out of 80 subjects. The heterogeneity of the disease process is transparent by looking at how the subjects are spread across the scatter plot.

Table 4

Fig. 4 gives the confusion matrix with a breakdown on how the subjects were classified into the different groups. The overall agreement for cluster and the clinical diagnosis for the four groups is 68.8%.

	cLA	cAD	cSIVD	cMX	Total	% Agreement
LA	11	0	4	1	16	68.8
AD	6	19	0	5	30	63.3
SIVD	2	0	13	3	18	72.2
MX	0	1	3	12	16	75
Total	19	21	20	20	80	68.8

3.3. Relationship with cognition

Executive function has significant negative spearman correlation with the VDS score (Fig. 8A) and the memory function has significant negative Spearman correlation with the ADS score (Fig. 8B) after correcting for age, sex, and education. The Pearson correlation (not indicated in the figure) had slightly stronger significance than the Spearman correlation. This correlation is based on including all the 80 patients and does not depend on the double-dichotomy clustering results. It should be noted that the reverse association is not true. In other words the VDS score is not correlated with the memory function and the ADS score is not correlated with the executive function. A subset of subjects ($n = 55$) was chosen where the clinical diagnosis and the cluster diagnosis were in agreement. In this group of subjects the executive function had a stronger negative correlation with the VDS score (Fig. 8C) and the memory function a stronger negative correlation with the ADS score (Fig. 8D).

4. Discussion

4.1. Calculation of normalized severity scores

We have shown that normalized severity scores not only provide objectivity in defining disease severity on a continuous basis, but also show the expected correlation with cognitive function. An OCC method was used to calculate these scores. Clustering of the reference/control class was used to define robust estimates of the mean and the covariance function. Although the severity scores were calculated based on only

two biomarkers each for the vascular and the AD pathways, the method can easily incorporate additional neuroinflammation and neurodegeneration biomarkers of the respective pathways. The present analysis was done based on whole brain MRI biomarkers, but it is equally possible to include regional measures such as hippocampal volume, functional connectivity [39], and blood-brain barrier permeability [21,40].

4.2. Dichotomy plot

The VDS and the ADS scores being based on biomarkers sensitive to two different processes were plotted orthogonally to get a two-dimensional scatter plot (Fig. 7). This plot showed the disease heterogeneity, a subject's position on the plot was an indication of disease type and severity, and by dividing the patients into four groups we were able to identify those with MX.

The ADS and the VDS score are summary biomarkers for the AD and the SIVD disease processes. Their calculation requires a well defined reference class, but does not require information of diagnostic groups and the method can be applied to other data sets. ADS and the VDS scores can themselves be treated as biomarkers, and in the future, classification can be done in terms of these variables. In other words, rather than using simple quadrants in Fig. 7 for separating groups, more complicated decision boundaries can be drawn.

4.3. Correlation with cognition

The VDS and ADS scores were only calculated based on physiological variable (MRI and CSF) and neuropsychological variables were intentionally not used. The fact that the VDS score was correlated to executive and the ADS score was correlated to the memory function, with the reverse not being true, gives additional credence to the fact these VDS and ADS scores depend on specific disease processes.

4.4. Selecting a subgroup of subjects

A subset of subjects with matching clinical and cluster diagnosis was selected. In this subset of subjects the correlation of the VDS score to the executive function and of the ADS score to the memory function was stronger than in the whole group. A biological biomarker based classification combined with clinical diagnosis identifies a smaller group of subjects with more consistent relationship with cognitive function. The objective classification complements the clinical diagnosis.

4.5. Advantages and limitations of the OCC method

The OCC method for clustering was selected based on its simplicity and minimal assumptions. The specific OCC method we chose, the MCD method, requires that the control class be unimodal and be defined by elliptical distributions. It does not place restrictions on the statistical distribution of outliers or subjects with different forms and severity of disease damage. We do not imply with our choice of the MCD method and the specific four biomarkers selected, that other more sophisticated classifications methods (such as random-forest) or alternate biomarkers, will not give better classification results. It should be noted, that if complex classification methods or a large number of biomarkers are used, then because of the limited number of subjects/groups in our pool, overfitting, even with cross-validation is a real possibility. Our goal was to show that double-dichotomy concept is useful, giving interpretable results with previously proven biomarkers.

One distinct advantage of the OCC method is that it can be applied to other data sets where AD-sensitive biomarkers are available for a control group, without the requirement of a clinical diagnosis similar to ours. The method requires a well-defined reference class, which can be subjects with mild cognitive impairment from other databases. A 2D-scatter plot with each axis representing disease severity can be obtained if we have data from one well-defined class, without the knowledge

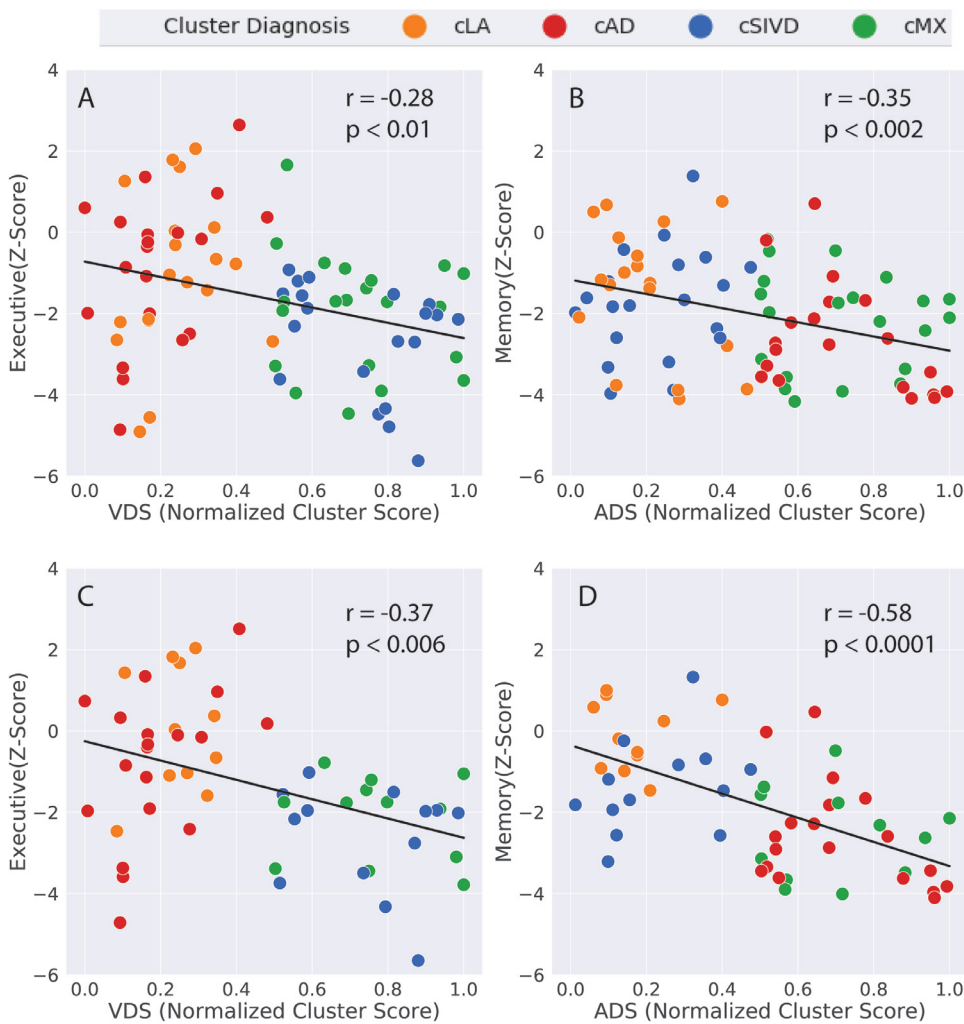


Fig. 8. The spearman correlation between the executive function and the VDS score and between the memory function and the ADS score for the full patient group (80 subjects) is shown in Figs. 8A and 8B, and for a subset of the subjects (55 subjects) in Figs. 8C and 8D. The selected subset of subjects for Figs. 8C and 8D are those with matching clinical and biomarker-based cluster diagnosis. In this subset of subjects there is stronger correlation with cognitive function. This is an example of how cluster diagnosis can be used to identify a more homogenous group of subjects with well characterized properties.

of disease groups. Any subsequent classification can be based on these plots.

4.6. Dependence on csf biomarkers

One limitation of the current example is the need for CSF-biomarkers for characterizing ADS. A number of laboratories are developing plasma based biomarkers for measurement of $A\beta$ ratio and pTau [41,42]. These biomarkers may supplant the CSF biomarkers we used and will make AD diagnosis practical for patients who cannot or will not undergo lumbar puncture. We also explored whether MRI markers such as hippocampal volume and brain atrophy could be used as surrogates for CSF markers, but results were considerably poorer.

4.7. Other comments

Harmonization of this method for datasets collected across multiple-sites with different types of subject populations, different methods of data collection, and different nomenclature for diagnosis requires more work. The proposed OCC method may be useful in this context because it only requires that we have a harmonized control or a reference group of subjects across sites.

We expect imperfect agreement with the cluster analysis and clinical diagnoses. The clinicians used some of the data included in the cluster measures. The cluster measure purposely left out subjective information used by the diagnosticians. Mismatches between the clinical and the cluster diagnoses were mainly of two types. The WMH from FLAIR was

used by the clinicians to determine white matter injury of presumed ischemic origin. Mismatches occurred when the PSMD was low and the WMH volume was high, leading to a lower white matter injury score for the cluster but higher salience to the clinician. Another mismatch occurred when clinicians used memory scores to identify AD patients. The most common discrepancy, with clinical AD sorting into cluster LA, may have resulted from older patients with memory deficits and CSF abnormality in only one of the two AD biomarkers contributing to ADS. The clinicians used cognitive function during their diagnosis and we have intentionally not treated cognition as biomarker, but as an outcome variable. However, current results are also notable for clinical-cluster consistency between AD and SIVD; no clinically diagnosed AD patient clustered in SIVD and vice versa (Table 4). Clustering, a relatively simple method for distinguishing groups, is successful only when the diagnostic categories are distinct, and the relatively high success when using only a few biomarkers illustrates that AD and the SIVD diagnostic categories are quite distinct, with categories having higher overlap (or "confusion", Table 4 and Fig. 7) indicating greater similarity in their presentation.

The age distribution of subjects in the different dementia subgroups was similar for the cluster and the clinical diagnosis. Subjects with MX, those having dual-pathology were identified at an older age (above 62 years) by both the clustering and the clinical diagnosis. This observation is also in agreement with the recent paper, that age related stratification AD and SIVD subjects becomes difficult at an older age because both AD and vascular dementia factors can co-exist [14]. Pathological changes begin at different ages with the accumulation of amyloid protein into plaques in mid-life, particularly in the genetic early onset forms

of the disease [43]. A parallel, but separate process is occurring in the blood vessels of hypertensive individuals; in mid-life there is a gradual increase in blood pressure, which, if untreated, continues to progress reaching a stage where the integrity of the white matter is compromised [9]. While these two processes are separate, they converge with aging and compound the injury to the brains of those with MX through a process of accelerated inflammation, leading to more severe cognitive loss. The ability with biomarkers to separate patients into AD, SIVD, and MX groups provides a means to begin to understand the timing of the onset of each process, which would allow selection of treatments at an earlier time point based on biomarker classification. Dementia studies have reached an impasse with the failure of a number of large clinical trials based on only the amyloid hypothesis. As novel mechanisms leading to dementia are discovered, new classes of treatments are being proposed; smaller more homogeneous cohorts would greatly facilitate these more complicated, multiagent trials [44].

Studies based on a neuropsychological endpoint will require 3 to 5 years for statistical validation, while other biomarkers, primarily derived from MRI, could show results in 1 to 2 years: the numbers of subjects would be greatly reduced with a more precise grouping of patients based on biological characteristics as shown by biomarkers, allowing studies with combination therapies [45]. Our results show that a machine-learning based biomarker-driven system could aid in selection of the smaller groups of homogeneous patients needed to assure success of studies in a reasonable time frame with combinations of drugs.

4.8. Limitation

The results of cluster diagnosis presented in this paper are limited, because they are based only on two biomarkers for each pathway. The method can easily incorporate other biomarkers, and if patients groups are well defined, and there are larger number of subjects, then more advanced classification methods, which include cross-validation to define appropriate decision boundaries can be used. Another similar limitation is that the severity scores depend on our control data sets. The harmonization of the severity scores and the decision boundaries for multi-site data sets requires further work. The MRI markers for the present work were global whole brain measures. It is possible that regional and fiber-tract dependent MRI measures have better prediction of cognition and may also serve as surrogate for CSF biomarkers. This also requires further work

5. Conclusions

We have proposed a method of constructing objective numerical indices of disease severity that can eventually be used to communicate results between different research and/or treatment centers. The method gives a continuous measure of disease severity instead of “mild”, “moderate”, and “severe” we get from clinicians. The orthogonal double-disctomy plot replaces the discrete four group classification used at our site with a continuous two-dimensional scatter plot. The continuous measures of severity were correlated to other continuous measures such as cognitive function scores to show that our scores are meaningful. The proposed method of calculating numeric severity scores based on biological biomarker can be used by clinicians to monitor the consistency of their diagnosis and for disease progression. This method can be further developed with applications to larger data sets, and also used to identify an optimal set of biomarkers, that are easier to measure, and robust with respect to clinical outcomes and diagnosis.

Author contributions

AC collected and analyzed the MRI data, constructed the cluster analysis, and wrote the first draft. RR and LH helped with MRI diffusion analysis and the python analysis scripts, JP performed the neuropsychological testing. JT did the measurements on the CSF samples. EE

provided statistical support in the interpretation of the data. JA, JK, and GR recruited the patients. GR designed the study, revised the draft, and obtained the funding.

Declaration of Competing Interest

There is no existing or potential conflict of interest for all authors associated with this research.

Acknowledgments

The authors acknowledge support from NIH grants UH3 NS100598 (MarkVCID), RO1 NS052305, and RO1 NS068048, and DHHS/NIH/NCRR #UL1TR001449.

References

- [1] P.B. Gorelick, A. Scuteri, S.E. Black, C. Decarli, S.M. Greenberg, C. Iadecola, et al., Vascular contributions to cognitive impairment and dementia: a statement for healthcare professionals from the american heart association/american stroke association, *Stroke* 42 (2011) 2672–2713.
- [2] V. Cipollini, F. Troili, F. Giubilei, Emerging biomarkers in vascular cognitive impairment and dementia: from pathophysiological pathways to clinical application, *Int. J. Mol. Sci.* 20 (11) (2019) 2812–2838.
- [3] C.R. Jack Jr., D.A. Bennett, K. Blennow, M.C. Carrillo, B. Dunn, S.B. Haeberlein, et al., NIA-AA Research Framework: toward a biological definition of Alzheimer's disease, *Alzheimers Dement.* 14 (2018) 535–562.
- [4] K. Dhiman, K. Blennow, H. Zetterberg, R.N. Martins, V.B. Gupta, Cerebrospinal fluid biomarkers for understanding multiple aspects of Alzheimer's disease pathogenesis, *Cell. Mol. Life Sci.* 76 (2019) 1833–1863.
- [5] C. Iadecola, The pathobiology of vascular dementia, *Neuron* 80 (2013) 844–866.
- [6] L. Pantoni, Cerebral small vessel disease: from pathogenesis and clinical characteristics to therapeutic challenges, *Lancet Neurol.* 9 (2010) 689–701.
- [7] J.M. Wardlaw, M.C. Valdes Hernandez, S. Munoz-Maniega, What are white matter hyperintensities made of? Relevance to vascular cognitive impairment, *J. Am. Heart Assoc.* 4 (2015) 001140.
- [8] E. Baykara, B. Gesierich, R. Adam, A.M. Tuladhar, J.M. Biesbroek, H.L. Koek, et al., A novel imaging marker for small vessel disease based on skeletonization of white matter tracts and diffusion histograms, *Ann. Neurol.* 80 (2016) 581–592.
- [9] P. Maillard, S. Seshadri, A. Beiser, J.J. Himali, R. Au, E. Fletcher, et al., Effects of systolic blood pressure on white-matter integrity in young adults in the Framingham Heart Study: a cross-sectional study, *Lancet Neurol.* 11 (2012) 1039–1047.
- [10] R. Koncz, P.S. Sachdev, Are the brain's vascular and Alzheimer pathologies additive or interactive? *Curr. Opin. Psychiatry* 31 (2018) 147–152.
- [11] N.A. Weaver, T. Doeve, F. Barkhof, J.M. Biesbroek, O.N. Groeneveld, H.J. Kuijff, et al., Cerebral amyloid burden is associated with white matter hyperintensity location in specific posterior white matter regions, *Neurobiol. Aging* 84 (2019) 225–234.
- [12] J. Graff-Radford, E.M. Arenaza-Urquijo, D.S. Knopman, C.G. Schwarz, R.D. Brown, A.A. Rabinstein, et al., White matter hyperintensities: relationship to amyloid and tau burden, *Brain* 142 (2019) 2483–2491.
- [13] G.A. Rosenberg, J. Prestopnik, J. Knoefel, J.C. Adair, J. Thompson, R. Raja, et al., A multimodal approach to stratification of patients with dementia: selection of mixed dementia patients prior to autopsy, *Brain Sci.* 9 (8) (2019) 187–196.
- [14] I.F. Jorgensen, A. Aguayo-Orozco, M. Lademann, S. Brunak, Age-stratified longitudinal study of Alzheimer's and vascular dementia patients, *Alzheimers Dement* (2020).
- [15] D.A. Snowden, L.H. Greiner, J.A. Mortimer, K.P. Riley, P.A. Greiner, W.R. Markesbery, Brain infarction and the clinical expression of Alzheimer disease. The Nun Study [see comments], *JAMA* 277 (1997) 813–817.
- [16] M.M. Esiri, Z. Nagy, M.Z. Smith, L. Barnettson, A.D. Smith, Cerebrovascular disease and threshold for dementia in the early stages of Alzheimer's disease [letter], *Lancet* 354 (1999) 919–920.
- [17] J.B. Toledo, S.E. Arnold, K. Raible, J. Brettschneider, S.X. Xie, M. Grossman, et al., Contribution of cerebrovascular disease in autopsy confirmed neurodegenerative disease cases in the National Alzheimer's Coordinating Centre, *Brain* 136 (2013) 2697–2706.
- [18] J.A. Schneider, Z. Arvanitakis, W. Bang, D.A. Bennett, Mixed brain pathologies account for most dementia cases in community-dwelling older persons, *Neurology* 69 (2007) 2197–2204.
- [19] J.A. Sonnen, K. Santa Cruz, L.S. Hemmy, R. Woltjer, J.B. Leverenz, K.S. Montine, et al., Ecology of the aging human brain, *Arch. Neurol.* 68 (2011) 1049–1056.
- [20] T. Erkinjuntti, Diagnosis and management of vascular cognitive impairment and dementia, *J. Neural Transm. Suppl.* 63 (2002) 91–109.
- [21] B.N. Huisa, G.A. Rosenberg, Binswanger's disease: toward a diagnosis agreement and therapeutic approach, *Expert Rev. Neurother.* 14 (2014) 1203–1213.
- [22] G.A. Rosenberg, A. Wallin, J.M. Wardlaw, H.S. Markus, J. Montaner, L. Wolfson, et al., Consensus statement for diagnosis of subcortical small vessel disease, *J. Cereb. Blood Flow Metab.* 36 (2016) 6–25.
- [23] G. McKhann, D. Drachman, M. Folstein, R. Katzman, D. Price, E.M. Stadlan, Clinical diagnosis of Alzheimer's disease: report of the NINCDS-ADRDA Work Group under the auspices of Department of Health and Human Services Task Force on Alzheimer's Disease, *Neurology* 34 (1984) 939–944.

- [24] G.M. McKhann, D.S. Knopman, H. Chertkow, B.T. Hyman, C.R. Jack Jr., C.H. Kawas, et al., The diagnosis of dementia due to Alzheimer's disease: recommendations from the National Institute on Aging-Alzheimer's Association workgroups on diagnostic guidelines for Alzheimer's disease, *Alzheimers Dement* 7 (2011) 263–269.
- [25] V.C. Hachinski, P. Potter, H. Merskey, Leuko-araiosis, *Arch. Neurol.* 44 (1987) 21–23.
- [26] M.D. Lezak, D.B. Howieson, E.D. Bigler, D.T. Neuropsychological Assessment, Oxford University Press, New York, 2012.
- [27] O. Spreen, E. S. A compendium of Neuropsychological tests: Administration, Norms and Commentary, Oxford University Press, New York, 1998.
- [28] J. Brandt, B. BRH, Hopkins Verbal Learning Test—Revised, Professional Manual, Psychological Assessment Resources, Lutz, FL, 2001.
- [29] S. Weintraub, L. Besser, H.H. Dodge, M. Teylan, S. Ferris, F.C. Goldstein, et al., Version 3 of the Alzheimer Disease Centers' neuropsychological test battery in the Uniform Data Set (UDS), *Alzheimer Dis. Assoc. Disord.* 32 (2018) 10–17.
- [30] S. Weintraub, D. Salmon, N. Mercaldo, S. Ferris, N.R. Graff-Radford, H. Chui, et al., The Alzheimer's Disease Centers' Uniform Data Set (UDS): the neuropsychologic test battery, *Alzheimer Dis. Assoc. Disord* 23 (2009) 91–101.
- [31] J.E. Meyers, K.R. Meyers, Rey Complex Figure Test and Recognition Trial, Psychological Assessment Resources, Odessa, FL, 1995.
- [32] D. Wechsler, Wechsler Memory Scale Revised, The Psychological Corporation, San Antonio, TX, 1987.
- [33] J. Patterson, F-A-S Test, in: J.S. Kreutzer, J. DeLuca, BC (Eds.), *Encyclopedia of Clinical Neuropsychology*, Springer, New York, NY, 2011.
- [34] R.M. Reitan, Validity of the trail making test as an indicator of organic brain damage, *Percept. Mot. Skills* 8 (1958) 271–276.
- [35] S.S. Khan, M.G. Madden, One-class classification: taxonomy of study and review of techniques, *Knowl. Eng. Rev.* 29 (2014) 345–374.
- [36] I. Irigoien, B. Sierra, C. Arenas, Towards application of one-class classification methods to medical data, *ScientificWorldJournal* 2014 (2014) 730712 -.
- [37] Y. Zhao, Z. Nasrullah, Z. Li, PyOD: a Python toolbox for scalable outlier detection, *J. Mach. Learn. Res.* 20 (2019) 1–7.
- [38] J. Hardin, D.M. Rocke, Outlier detection in the multiple cluster setting using the minimum covariance determinant estimator, *Comput. Stat. Data Anal.* 44 (2004) 625–638.
- [39] Z. Fu, A. Iraj, A. Caprihan, J.C. Adair, J. Sui, G.A. Rosenberg, et al., In search of multimodal brain alterations in Alzheimer's and Binswanger's disease, *Neuroimage Clin* (2019) 101937.
- [40] G.A. Rosenberg, Inflammation and white matter damage in vascular cognitive impairment, *Stroke* 40 (2008) S20–S23.
- [41] F.M. Elahi, K.B. Casaletto, R. La Joie, S.M. Walters, D. Harvey, A. Wolf, et al., Plasma biomarkers of astrocytic and neuronal dysfunction in early- and late-onset Alzheimer's disease, *Alzheimers Dement* 16 (2020) 681–695.
- [42] T.K. Karikari, T.A. Pascoal, N.J. Ashton, S. Janelidze, A.L. Benedet, J.L. Rodriguez, et al., Blood phosphorylated tau 181 as a biomarker for Alzheimer's disease: a diagnostic performance and prediction modelling study using data from four prospective cohorts, *Lancet Neurol.* 19 (2020) 422–433.
- [43] P.H. Luckett, A. McCullough, B.A. Gordon, J. Strain, S. Flores, A. Dincer, et al., Modeling autosomal dominant Alzheimer's disease with machine learning, *Alzheimers Dement* (2021).
- [44] J.M. Long, D.M. Holtzman, Alzheimer disease: an update on pathobiology and treatment strategies, *Cell* 179 (2019) 312–339.
- [45] P. Benjamin, E. Zeestraten, C. Lambert, I.C. Ster, O.A. Williams, A.J. Lawrence, et al., Progression of MRI markers in cerebral small vessel disease: sample size considerations for clinical trials, *J. Cereb. Blood Flow Metab.* 36 (2016) 228–240.
- [46] V.C. Hachinski, Multi-infarct dementia: a reappraisal, *Alzheimer Dis Assoc Disord* 5 (1991) 64–68.